JOURNAL OF MATERIALS SCIENCE 32 (1997) 1937–1942

High temperature strength and oxidation behaviour of hot-pressed silicon nitride-disilicate ceramics

HEON-JIN CHOI, JUNE-GUNN LEE
Division of Ceramics, Korea Institute of Science and Technology P.O. Box 131 Cheongryang, Seoul 130-650, Korea

YOUNG-WOOK KIM
Department of Materials Science and Engineering, Seoul City University, 90 Jeonnong-Dong, Dongdaemoon-Gu, Seoul 130-743, Korea

Twelve different silicon nitride-disilicate ceramics have been fabricated by hot-pressing Si_3N_4 with the oxides of Y, Yb, Ho, Dy, Er, Sm, Ce, Lu, La, Pr, Gd, and Sc that are used as sintering additives. The high temperature strength and oxidation behaviour of the hot-pressed ceramics were investigated and correlated with the cationic radii of the oxide additives. The flexural strength at 1200 °C increased, from 666 MPa for Si_3N_4–$La_2Si_2O_7$ to 965 MPa for Si_3N_4–$Sc_2Si_2O_7$ which is correlated with a decreasing cationic radius of the oxide additive. The weight gain during oxidation at 1400 °C for 192 h in air decreased, from 0.8732 mg cm^{-2} for a Si_3N_4–$Sm_2Si_2O_7$ ceramic to 0.1089 mg cm^{-2} for a Si_3N_4–$Sc_2Si_2O_7$ ceramic, which is a function of the decreasing cationic radius of the oxide additive.

1. Introduction

Silicon nitride (Si_3N_4) contains a high degree of covalent bonding and does not decompose until ~ 1880 °C. Therefore, it is impossible to densify Si_3N_4 without the use of sintering additives. Densification is achieved by liquid-phase sintering usually using metal oxides such as MgO, Al_2O_3, and Y_2O_3 as the sintering additives. These oxides react with SiO_2, which is always present at the surface of Si_3N_4 particles, to form an oxide melt and with increasing temperature, an oxynitride melt with the dissolution of Si_3N_4.

A problem associated with the use of additives is the resultant degradation of high temperature properties due to residual grain boundary glassy phases [1, 2]. Several attempts to prevent the observed degradation in the high temperature properties have been reported. These include the tailoring of the grain boundary glassy phases [3], crystallizing the grain boundary glassy phases [4], and using transient liquid phase sintering [5].

Work performed by Lange *et al.* [6] on the Si_3N_4–SiO_2–Y_2O_3 system has shown that the high temperature properties of Si_3N_4 can be improved by choosing compositions in the Si_3N_4–Si_2N_2O–$Y_2Si_2O_7$ compatibility triangle, since the Si_2N_2O and $Y_2Si_2O_7$ phases are in equilibrium with SiO_2 (the oxidation product of Si_3N_4). Lange [7] also proposed similar behaviour for compositions in the Si_3N_4–SiO_2–Ce_2O_3 system. On this basis, various rare earth oxides have been studied as potential sintering additives, since it is expected that Si_3N_4–SiO_2–rare earth oxide systems would also exhibit this type of behaviour. It has been shown that rare earth oxides are as effective as Y_2O_3 in the densification of Si_3N_4 [4, 8, 9]. Furthermore, refractory disilicate, $RE_2Si_2O_7$ (RE refers to the cation of a rare earth oxide), can be crystallized at grain boundaries, thereby resulting in improved high temperature properties [4, 10, 11]. In the ideal case complete crystallization of the grain boundary phases occurs, however, it has been proposed, based on thermodynamic considerations [12] and transmission electron microscopy observations [4, 13], that a thin residual glassy film always exists at the grain boundary. Therefore, the selection of a highly refractory grain boundary glassy phase could be an effective means for achieving improved high temperature properties [10, 11].

The objective of this study was to investigate the effect of an oxide additive, M_xO_y (M refers to the cations of Y_2O_3, Yb_2O_3, Ho_2O_3, Dy_2O_3, Er_2O_3, Sm_2O_3, CeO_2, Lu_2O_3, La_2O_3, Pr_6O_{11}, Gd_2O_3, and Sc_2O_3), on the high temperature strength and oxidation resistance of Si_3N_4 ceramics. Twelve different Si_3N_4-disilicate ($M_2Si_2O_7$) ceramics were fabricated by hot-pressing and their high temperature flexural strength and oxidation behaviour were investigated.

2. Experimental procedure

Commercially available Si_3N_4 (SN E-10, Ube Industries, Tokyo, Japan) and the oxide additives were used for fabricating the Si_3N_4–$M_2Si_2O_7$ ceramics. The

0022–2461

TABLE I Compositions and properties of the Si_3N_4–$M_2Si_2O_7$ ceramics

Material	Si_3N_4–SiO_2[a]–M_xO_y (mol %)	Relative density (%)	Flexural strength at 1200 °C (MPa)	Weight gain at 1400 °C for 192 h (mg cm^{-2})
Si_3N_4–$Y_2Si_2O_7$	84.9–10.6–5.4	99.7	893	0.2799
Si_3N_4–$Yb_2Si_2O_7$	83.3–11.2–5.5	99.9	754	0.4129
Si_3N_4–$Ho_2Si_2O_7$	83.8–10.7–5.5	99.3	767	0.8164
Si_3N_4–$Dy_2Si_2O_7$	83.9–10.8–5.3	97.8	752	0.2318
Si_3N_4–$Er_2Si_2O_7$	83.7–10.8–5.5	97.7	762	0.1342
Si_3N_4–$Sm_2Si_2O_7$	85.3–9.4–5.4	98.2	726	0.8732
Si_3N_4–$Ce_2Si_2O_7$	81.8–12.2–6.0	98.7	755	0.2553
Si_3N_4–$Lu_2Si_2O_7$	83.4–11.2–5.4	96.5	954	0.2673
Si_3N_4–$La_2Si_2O_7$	84.4–11.2–5.4	98.5	666	0.3046
Si_3N_4–$Pr_2Si_2O_7$	88.2–10.0–1.8	98.5	737	0.4019
Si_3N_4–$Gd_2Si_2O_7$	84.2–10.5–5.3	99.3	665	0.3871
Si_3N_4–$Sc_2Si_2O_7$	83.7–11.7–4.6	99.9	965	0.1089

[a] Taking into account SiO_2 on the surface of the Si_3N_4 particles

oxide additives were SiO_2 (99.9%, Aerosil 200, Degussa Corp., NJ, USA) and twelve M_xO_y (Y_2O_3, Yb_2O_3, Ho_2O_3, Dy_2O_3, Er_2O_3, Sm_2O_3, CeO_2, Lu_2O_3, La_2O_3, Pr_6O_{11}, Gd_2O_3, and Sc_2O_3, 99.9%, Johnson Matthey, Seabrook, NH, USA). All the compositions were prepared with a molar ratio of $SiO_2 : M_xO_y$ correspond to the Si_3N_4–$M_2Si_2O_7$ tie line (Table 1). The SiO_2 content present on the surface of the Si_3N_4 particles was taken from the manufacturer's data to be 2.6 wt % (3.1 vol %). The total amount of the sintering additives was fixed at 12 vol %. The powder mixtures were milled in methanol for 24 h using Si_3N_4 grinding balls. The milled slurry was dried, sieved, and hot-pressed at 1820 °C for 2 h at an applied pressure of 25 MPa under a nitrogen atmosphere.

Sample densities were measured using the Archimedes method. The theoretical densities of the specimens were calculated according to the rule of mixtures. Crystalline phases in the sintered specimens were determined by X-ray diffraction (XRD) using CuK_α radiation. Flexural test specimens were cut into $3 \times 2.5 \times 20$ mm bars from hot-pressed disc samples, and their surfaces and edges polished with an 800-grit diamond wheel. The flexural strength values were measured at 1200 °C by a three-point bending method with a span of 15 mm. The hot-pressed specimens were cut and polished, and then etched using molten NaOH. The microstructures were observed by scanning electron microscopy (SEM) and the SEM micrographs were analysed by image analysis (MAGISCAN, Joyce Loeble, UK). The diameter and length of each grain were directly determined from the shortest and longest grain diagonal, respectively. The aspect ratio of each grain was estimated as the ratio of length to diameter. A total of between 800 to 1000 grains were used for statistical analysis of each specimen. To test for oxidation resistance $18 \times 18 \times 2.5$ mm specimens were cut and polished, placed on platinum wire in a box furnace, heated to 1400 °C at a heating rate of 450 °C h^{-1}, and held at temperature for 192 h. The furnace was cooled and heated between 12–72 h intervals in order to measure weight changes in the specimens.

3. Results

The characteristics of the Si_3N_4–$M_2Si_2O_7$ ceramics are summarized in Table I. The relative densities of $\geq 96.5\%$ were achieved by hot-pressing with a holding time of 2 h at 1820 °C. The highest densities of 99.9% were obtained for the Si_3N_4–$Sc_2Si_2O_7$ and Si_3N_4–$Yb_2Si_2O_7$ ceramics, and the lowest density of 96.5% was obtained for the Si_3N_4–$Lu_2Si_2O_7$ ceramic. XRD of the specimens showed β-Si_3N_4 as the major phase and $M_2Si_2O_7$ as the minor phase in every specimen.

The microstructures of the Si_3N_4–$M_2Si_2O_7$ ceramics are shown in Fig. 1(a–l). The microstructures of the Si_3N_4–$Ho_2Si_2O_7$, Si_3N_4–$Er_2Si_2O_7$, and Si_3N_4–$Gd_2Si_2O_7$ ceramics appear to have a greater amount of the residual glassy phase as compared to the others. The microstructures of the Si_3N_4–$Sc_2Si_2O_7$ and Si_3N_4–$Ho_2Si_2O_7$ ceramics appear to have a more pronounced grain growth of β-Si_3N_4, which is known to enhance mechanical properties. The results of the application of image analysis to the micrographs are summarized in Table II. The average diameters ranged from 0.31 μm for Si_3N_4–$Yb_2Si_2O_7$ to 0.50 μm for Si_3N_4–$Dy_2Si_2O_7$ whilst the average aspect ratio ranged from 1.98 for Si_3N_4–$Y_2Si_2O_7$ to 2.32 for Si_3N_4–$Ho_2Si_2O_7$. Hoffman [14] has reported that the average aspect ratio of β-Si_3N_4 grains decreases with a decreasing cationic radius of rare earth and yttrium oxide additives (Yb, Gd, Nd, La, and Y). However, Cinibulk and Thomas [4] obtained similar microstructures for Si_3N_4 doped with various kinds of rare earth and yttrium oxide additives (Sm, Gd, Dy, Er, Yb, and Y). Sanders and Mieskowski [8] also reported that the addition of Y_2O_3 produced a higher area fraction of elongated grains (β-Si_3N_4) than the addition of Ce_2O_3, Sm_2O_3, and La_2O_3, although the cationic radius of Y is smaller than the others. No dependence of the microstructure on the cationic radius of the oxide additives has been observed in the present study. The discrepancy between previously reported data and the present results indicate that the cationic radii of the oxide additives may not be the dominant parameter in the microstructural evolution of Si_3N_4.

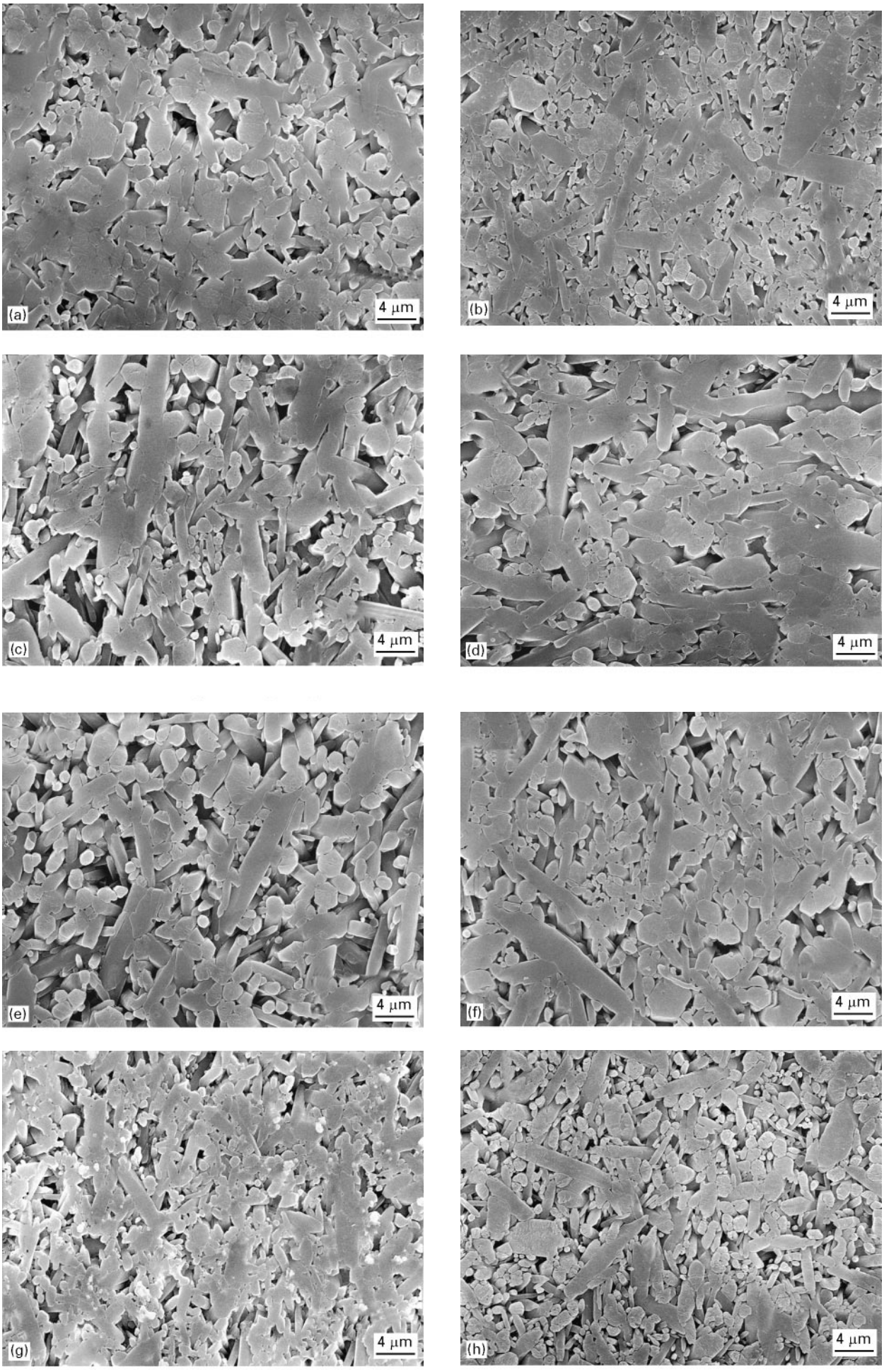

Figure 1 Scanning electron micrographs of the polished and etched Si_3N_4–$M_2Si_2O_7$ ceramics for (a) Y, (b) Yb, (c) Ho, (d) Dy, (e) Er, (f) Sm, (g) Ce, (h) Lu, (i) La, (j) Pr, (k) Gd and (l) Sc.

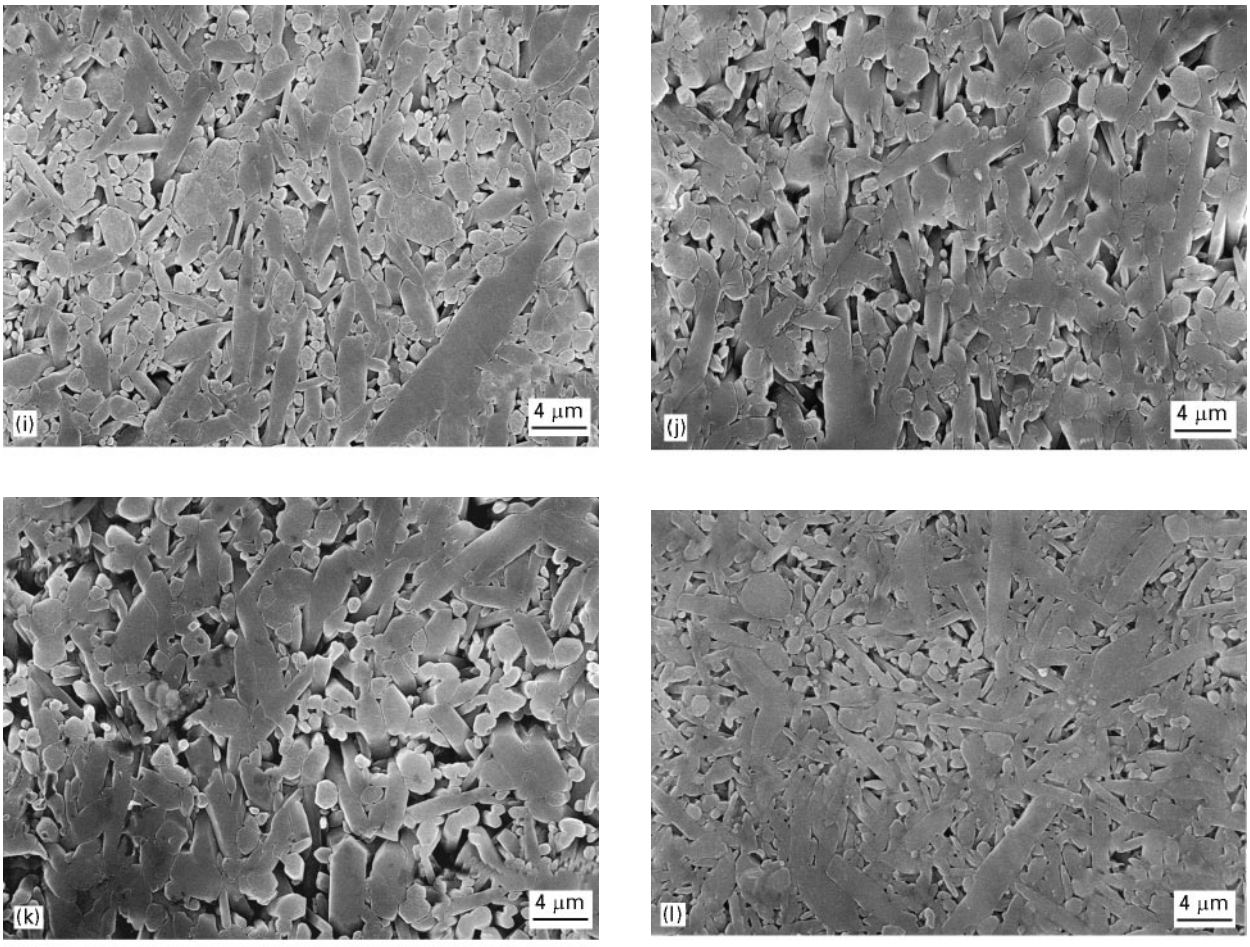

Figure 1 (Continued).

TABLE II Average grain diameters and aspect ratios of the Si_3N_4–$M_2Si_2O_7$ ceramics

Material	Average diameter (μm)	Average aspect ratio
Si_3N_4–$Y_2Si_2O_7$	0.39	1.98
Si_3N_4–$Yb_2Si_2O_7$	0.31	2.09
Si_3N_4–$Ho_2Si_2O_7$	0.43	2.32
Si_3N_4–$Dy_2Si_2O_7$	0.50	2.09
Si_3N_4–$Er_2Si_2O_7$	0.48	2.26
Si_3N_4–$Sm_2Si_2O_7$	0.44	2.27
Si_3N_4–$Ce_2Si_2O_7$	0.32	2.16
Si_3N_4–$Lu_2Si_2O_7$	0.36	2.11
Si_3N_4–$La_2Si_2O_7$	0.41	2.07
Si_3N_4–$Pr_2Si_2O_7$	0.43	2.29
Si_3N_4–$Gd_2Si_2O_7$	0.45	2.07
Si_3N_4–$Sc_2Si_2O_7$	0.36	2.28

The flexural strengths measured at 1200 °C on sintered specimens are also presented in Table I. Three ceramics, Si_3N_4–$Lu_2Si_2O_7$, Si_3N_4–$Y_2Si_2O_7$, and Si_3N_4–$Sc_2Si_2O_7$, showed higher strength values (> 800 MPa) as compared to the others. The highest strength of 965 MPa was obtained for the Si_3N_4–$Sc_2Si_2O_7$ sample. Two ceramics, Si_3N_4–$La_2Si_2O_7$ and Si_3N_4–$Gd_2Si_2O_7$, showed lower strength values (< 700 MPa) as compared to the others. It is extensively documented that the interlocking of elongated grains due to the pronounced grain growth of β-Si_3N_4 increases the strength of Si_3N_4 [15]. Within the range studied, i.e., for the twelve Si_3N_4–$M_2Si_2O_7$ ceramics, the high temperature strength, however, was not dependent on the microstructure, i.e., the aspect ratio and diameter of the β-Si_3N_4 grains. For example, Si_3N_4–$Dy_2Si_2O_7$ has the largest diameter of 0.50 μm but also has a lower strength than Si_3N_4–$Sc_2Si_2O_7$ and Si_3N_4–$Lu_2Si_2O_7$ ceramics. Also Si_3N_4–$Pr_2Si_2O_7$ has the highest aspect ratio of 2.29 but also a lower strength than Si_3N_4–$Sc_2Si_2O_7$ and Si_3N_4–$Lu_2Si_2O_7$ ceramics. The variation of the high temperature strength with the radius of the cation in the oxide additive is shown in Fig. 2. The cationic radii used in this study are listed in Table III. As shown, the high temperature strength of Si_3N_4–$M_2Si_2O_7$ ceramics is strongly dependent on the cationic radius of the oxide additive.

Fig. 3 shows the relation between the square of the weight gain and oxidation time at 1400 °C. The oxidation behaviour of sintered specimens obeys a parabolic rate law of the type;

$$W^2 = kt \quad (1)$$

where W is the weight gain per unit surface area, k is the rate constant of parabolic oxidation, and t is the exposure time. The observed weight gains of sintered specimens after oxidation at 1400 °C for 192 h are also listed in Table I. Si_3N_4–$Sc_2Si_2O_7$ and Si_3N_4–$Er_2Si_2O_7$ ceramics showed weight gains lower than 0.2 mg cm^{-2} whereas Si_3N_4–$Ho_2Si_2O_7$ and Si_3N_4–$Sm_2Si_2O_7$ ceramics showed weight gains greater than 0.8 mg cm^{-2}. It was also observed that the weight gain

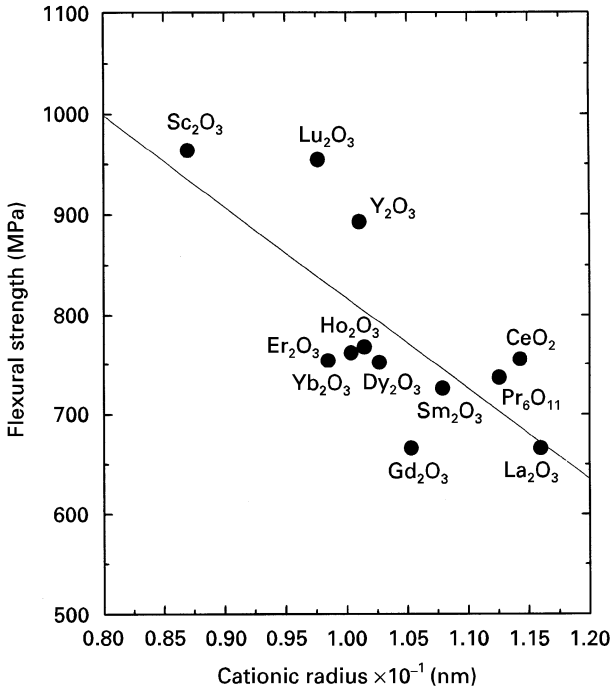

Figure 2 Relation between flexural strength at 1200 °C and cationic radius of M_xO_y additives for Si_3N_4–$M_2Si_2O_7$ ceramics.

TABLE III Cationic radii of the M_xO_y additives [16, 17] used in the present study

Additive	Cationic radius × 10^{-1} (nm)
Y_2O_3	1.011
Yb_2O_3	0.985
Ho_2O_3	1.015
Dy_2O_3	1.027
Er_2O_3	1.004
Sm_2O_3	1.079
CeO_2	1.143
Lu_2O_3	0.977
La_2O_3	1.160
Pr_6O_{11}	1.126
Gd_2O_3	1.053
Sc_2O_3	0.870

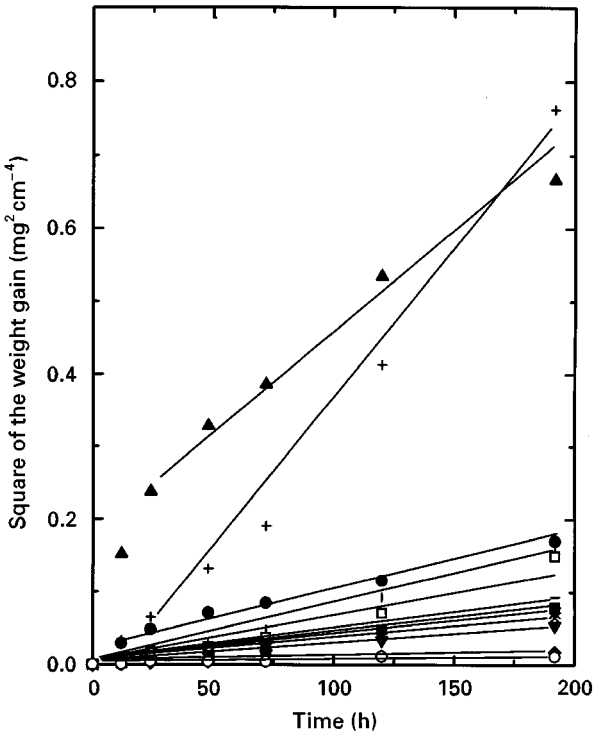

Figure 3 Relation between the square of weight gain at 1400 °C and time for Si_3N_4–$M_2Si_2O_7$ ceramics, where; (■) Y_2O_3, (●) Yb_2O_3, (▲) Ho_2O_3, (▼) Dy_2O_3, (◆) Er_2O_3, (+) Sm_2O_3 (×) CeO_2, (*) Lu_2O_3, (—) La_2O_3, (|) Pr_6O_{11}, (□) Gd_2O_3 and (○) Sc_2O_3.

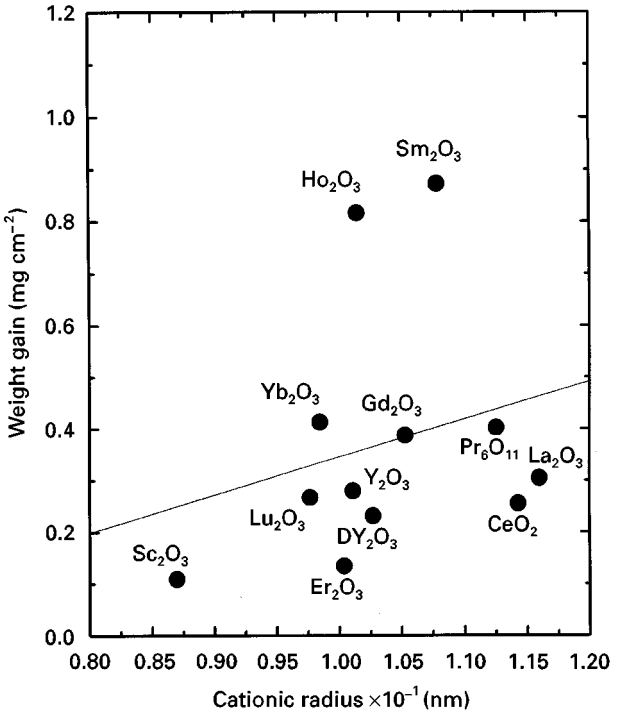

Figure 4 Relation between specific weight gain at 1400 °C and cationic radius of M_xO_y additives for Si_3N_4–$M_2Si_2O_7$ ceramics.

of the specimens during oxidation were dependent on the cationic radius of the oxide additives (Fig. 4). As shown, in general the weight gain decreased with a decreasing cationic radius with the exception of the Si_3N_4–$Sm_2Si_2O_7$ and Si_3N_4–$Ho_2Si_2O_7$ ceramics. The higher weight gain of the Si_3N_4–$Sm_2Si_2O_7$ ceramics has been previously reported by other investigators [11, 18]. It may be due to the aliovalent character of Sm, i.e., Sm exists in the divalent or trivalent state. The diffusion rate of divalent Sm is expected to be much greater than that of trivalent Sm [19] which would account for the much greater weight gain during oxidation. A similar explanation could be given for the higher weight gain of Si_3N_4–$Ho_2Si_2O_7$ ceramics.

4. Discussion

Since all the Si_3N_4 grains are completely wetted by the grain boundary phase [20], the high temperature properties, such as strength and oxidation resistance, of Si_3N_4 ceramics are predominantly determined by the refractory behaviour of the amorphous grain boundary phase, which is necessary for densification via liquid phase sintering. In turn, the refractory nature of the grain boundary phase strongly depends on the chemistry of the amorphous grain boundary phase.

The limited number of studies performed on silica-based glasses have shown that the rare earth oxides behave as a glass former in the glass structure [21, 22]. Thus, the cation in the rare earth oxides acts as a glass modifier in the SiO_4^{4-} tetrahedron since their size is larger than that of the Si ion (0.026 nm) [16]. In general, the physical properties of a glass are predominantly controlled by the bond strength between cations (Si ion or the cation of the oxide additive) and anions (oxygen ion). The bond strength is characterized as a "field strength" which is proportional to the ionic charge and the reciprocal of the ion size [23];

$$F_c = \frac{Z_a e \, Z_c e}{a^2} \quad (2)$$

where F_c is the field strength, Z_a is the charge of the anion, Z_c is the charge of the cation, e is the elementary electric charge, and a is the distance between the centre of two ions. The high temperature properties of a SiO_2 glass are believed to be determined by the weakest bond. Shelby and Kohli [24] showed that a bond between a cation of the additive and the surrounding oxygen ions is the weakest link in the SiO_2 glass structure because the cationic radius of the additive is the largest and the field strength is the weakest. They also observed that the physical properties, such as softening temperature and glass transition temperature, of an aluminosilicate glass increased linearly with decreasing cationic radius of the rare earth oxide additives. Therefore, the bond strength between the cation of the oxide additive and the oxygen ion is expected to increase with a decreasing cationic radius of the oxide additive.

A greater refractory nature of the amorphous grain boundary phase, hence, is expected for the Si_3N_4 ceramics sintered with the oxide additives having a smaller cationic radius. Consequently, the high temperature strength and oxidation resistance of the Si_3N_4–$M_2Si_2O_7$ ceramics in the present study were considered to improve with a decrease in the cationic radius of the oxide additive. These results suggest that the high temperature properties of Si_3N_4 ceramics might be improved by adding an oxide additive having a small cationic radius.

5. Conclusion

The flexural strength at 1200 °C and oxidation resistance at 1400 °C in the twelve Si_3N_4–$M_2Si_2O_7$ ceramics increased with a decrease in the cationic radius of the oxide additive. These results were attributed to the increasing bond strength between the cation of the oxide additives and oxygen ions within the amorphous grain boundary phase produced by a decrease in the cationic radius of the oxide additives. The present results suggest that oxide additives with a small cationic radius may be desirable to produce Si_3N_4 ceramics with improved properties at elevated temperatures.

References

1. J. L. ISKOE, F. F. LANGE and E. S. DIAZ, *J. Mater. Sci.* **11** (1976) 908.
2. S. C. SINGHAL, *ibid.* **11** (1976) 500.
3. D. P. THOMPSON, in Proceedings of the Material Research Society Symposium, Boston MA, December 1992, edited by I. W. Chen, P. F. Becher, M. Mitomo, G. Petzow and T. S. Tien (Materials Research Society, Pittsburg PA 1993). p. 79.
4. M. K. CINIBULK and G. THOMAS, *J. Amer. Ceram. Soc.* **75** (1992) 2037.
5. C. J. HWANG, S. M. FULLER and D. R. BEAMAN, *Ceram. Engng Sci. Proc.* **15** (1994) 685.
6. F. F. LANGE, S. C. SINGHAL and R. C. KUZNICKI, *J. Amer. Ceram. Soc.* **60** (1977) 249.
7. F. F. LANGE, *Amer. Ceram. Soc. Bull.* **59** (1980) 239.
8. W. A. SANDERS and D. M. MIESKOWSKI, *ibid* **64** (1985) 304.
9. N. HIROSAKI, A. OKADA and K. MATOBA, *J. Amer. Ceram. Soc.* **71** (1988) C-144.
10. M. K. CINIBULK and G. THOMAS, *ibid.* **75** (1992) 2050.
11. *Idem.*, *ibid.* **75** (1992) 2044.
12. D. R. CLARKE, *ibid.* **70** (1987) 15.
13. H. J. KLEEBE, M. K. CINIBULK, R. M. CANNON and M. RUHLE, *ibid.* **76** (1993) 1969.
14. M. J. HOFFMAN, in Proceedings of the NATO Advanced Research Workshop on Tailoring of High Temperature Properties of Si_3N_4 Ceramics, Münich, October 1993, edited by M. J. Hoeffman and G. Petzow (Kluwer Academic Publishers, Dordrecht, Netherlands, 1994) p. 59.
15. F. F. LANGE, *J. Amer Ceram. Soc.* **56** (1973) 518.
16. R. D. SHANNON, *Acta Cryst.* **A32** (1976) 751.
17. D. J. KIM, S. H. HYUN, S. G. KIM and M. YASHIMA, *J. Amer. Ceram. Soc.* **77** (1994) 597.
18. D. M. MIESKOWSKI and W. A. SANDERS, *ibid.* **68** (1985) C-160.
19. F. A. COTTON and G. WILKINSON, in "Advanced Inorganic Chemistry", 5th Edn (Wiley-Interscience, New York, 1988).
20. M. J. HOFFMAN, *MRS Bull.* **20** (1995) 28.
21. A. MAKISHIMA, Y. TAMURA and T. SAKAINO, *J. Amer. Ceram. Soc.* **61** (1978) 247.
22. A. MAKISHIMA, M. KOBAYASHI and T. SHIMOHIRA, *ibid.* **65** (1982) C-210.
23. A. DIETZEL, *Z. Elektrochem.* **48** (1942) 9.
24. E. SHELBY and J. T. KOHLI, *J. Amer. Ceram. Soc.* **73** (1990) 39.

Received 27 January 1995
and accepted 8 October 1996